THE JOURNAL OF PHYSICAL CHEMISTRY A

Article

Cite This: J. Phys. Chem. A 2018, 122, 6176−6182

pubs.acs.org/JPCA

Electronic Structure and Rydberg−Core Interactions in Hydroxycarbene and Methylhydroxycarbene

Published as part of The Journal of Physical Chemistry virtual special issue "William M. Jackson Festschrift".

Bibek R. Samanta, Subhasish Sutradhar, Ravin Fernando, Anna I. Krylov,* and Hanna Reisler*

Department of Chemistry, University of Southern California, Los Angeles, California 90089-0482, United States

Supporting Information

ABSTRACT: Vertical and adiabatic excitation energies and oscillator strengths for valence and Rydberg states of hydroxycarbene (HCOH) and methylhydroxycarbene (CH_3COH) are reported. The electronic properties were computed with equation-of-motion coupled-cluster methods with single and double substitution methods (EOM-CCSD) and the aug-cc-pVTZ basis set. The states' characters were analyzed by plotting natural transition orbitals (NTOs). The calculations demonstrate that the shape, size, and energy of each Rydberg orbital are affected to varying degrees by their interaction with the ion core. Likewise, the corresponding quantum defects reflect the Rydberg electron−ion core interactions. The results reported herein, combined with previously reported calculations of the photoelectron spectrum of HCOH, should help in designing strategies for state-selective detection of hydroxycarbenes via ionization.

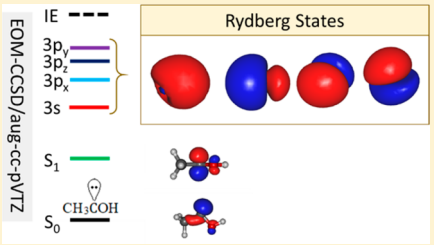

1. INTRODUCTION

Singlet carbenes, with their divalent carbon and a doubly occupied lone pair, are important reactants in synthetic chemistry.[1,2] Hydroxycarbenes, the tautomers of aldehydes, are known to be particularly reactive and therefore are difficult to isolate and study. These carbenes have been implicated early on in the synthesis of carbohydrates in space through photocatalysis.[3] Hydroxycarbenes have also generated much interest as high-lying intermediates in the excited-state dynamics of aldehydes.[4,5] The simplest member of the series, hydroxycarbene (HCOH), became the focal point of theoretical attention over 30 years ago as a possible participant in the unimolecular decomposition of formaldehyde.[6−10] More recent research involving the H_2CO/HCOH system was driven by experimental results that identified a roaming mechanism in the photodissociation of formaldehyde to CO + H_2.[11−13] These experiments inspired further theoretical work, including the generation of an accurate potential energy surface (PES) that encompasses these two tautomers, the CO + H_2 and H + HCO product channels, and the relevant transition states connecting them.[5,14−18] Moreover, the T_1/S_0 minimum energy crossing configuration in formaldehyde was found to occur at nuclear configurations similar to that of the transition state separating ground-state *cis*- and *trans*-HCOH.[16] In addition, trajectories starting from this crossing point and terminating in CO + H_2 were shown to sample the *cis*- and *trans*-HCOH wells before finding the much deeper H_2CO well from which they eventually proceeded to products. A more recent theoretical paper from the Bowman group treated also tunneling from *trans*-HCOH to H_2CO on this PES.[14]

Because of their high reactivity, hydroxycarbenes have been difficult to isolate for detailed studies of their photophysics and photochemistry. Reisler and co-workers generated HCOH in the gas-phase photodissociation of CH_2OH via the H + HCOH channel and characterized its internal states from the kinetic energy distributions of the H atom cofragments.[19−22] They also discovered that when HCOH is produced with sufficient internal energy, it undergoes decomposition either by O−H bond cleavage or via isomerization to formaldehyde.

Schreiner and co-workers succeeded in trapping hydroxycarbene (henceforth referred to as HC) and methylhydroxycarbene (MHC) in an argon matrix, and probing them by absorption spectroscopy.[23,24] Their experiments validated the existence of a high potential barrier to isomerization to the respective aldehydes. Furthermore, in a joint experimental and theoretical study, they found that the lifetimes were limited by H atom tunneling through the barrier to form the aldehydes. Lifetimes of 2 and 1 h were measured for HC and MHC, respectively.[23,24] The infrared (IR) vibrational spectra of HC and MHC, reported by the same authors, were in good agreement with a later study carried out in He nanodroplets.[25] Koziol et al. computed the IR spectra of *cis*- and *trans*-HC by accurate vibrational configuration interaction calculations.[26]

Schreiner and co-workers carried out electronic structure calculations of HC and MHC. The electronic energy differences computed at the ground and S_1 excited-state geometries agreed well with their observations of the ultraviolet (UV) absorption spectra to S_1.[23,24] Ionization of HC and MHC was studied theoretically, and vertical and

Received: May 9, 2018
Revised: June 28, 2018
Published: June 29, 2018

DOI: 10.1021/acs.jpca.8b04424
J. Phys. Chem. A 2018, 122, 6176−6182

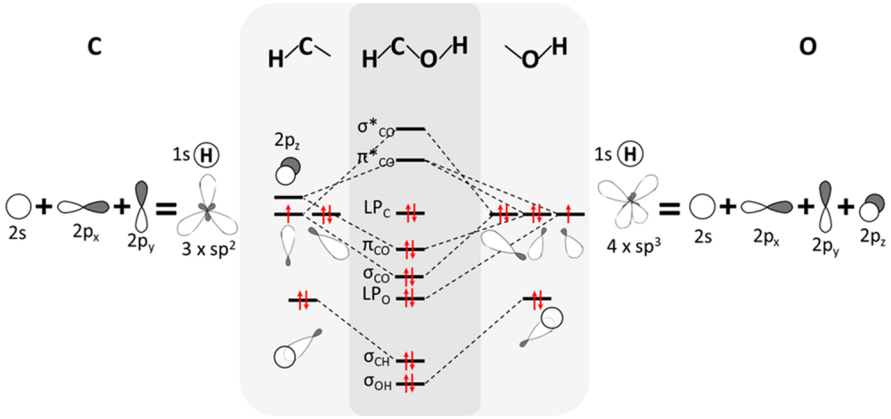

Figure 1. Molecular orbital diagram for *trans*-HC. The sp^2 hybridized C atom orbitals are shown on the left, and the sp^3 hybridized O atom orbitals are shown on the right. LP: lone pair. LP_C is the sp^2 hydridized carbon orbital in the *Y*-direction, which does not mix with any other orbital. LP_O is formed from two of the sp^3 hydridized orbitals on oxygen.

adiabatic energies were reported.[27] In addition, Koziol et al. computed the photoelectron spectra of *cis*- and *trans*-HC.[28]

Decarboxylation of α-keto acids such as glyoxylic acid and pyruvic acid has proven to be a reliable source of HC and MHC, respectively, especially for spectroscopic studies.[23−25,29−32] However, challenges remain in generating, isolating, and detecting these intermediates in the collisionless environment of molecular beams and in studying their dissociation dynamics. Resonance enhanced multiphoton ionization (REMPI) detection via Rydberg states is known to be a sensitive and state-selective detection method in molecular beams. Hydroxycarbenes should have several Rydberg states centered on carbon in addition to the S_1 states described above; these can be used to facilitate state-selective REMPI detection.

In this paper we report electronic structure calculations of electronically excited states of the first two members of the hydroxycarbene family, namely, the *cis*- and *trans*-isomers of HC and MHC. We find that above the S_1 state and below the ionization threshold, HC and MHC have several Rydberg states. The presence of an additional methyl group in MHC alters the charge distributions and excitation and ionization energies in predictable ways. To aid in the qualitative understanding of the nature of the Rydberg states and their electron−ion core interactions, we computed also natural transition orbitals (NTOs). Further information on the oscillator strengths and the direction of the transition dipole moments, which is useful in designing detection schemes, is gained from the shapes of the orbitals involved in the transitions and their symmetries. We discuss these orbital shapes and how they relate to the computed excitation energies. We end by considering possible experimental detection schemes for HC and MHC.

2. COMPUTATIONAL DETAILS

We optimized ground-state geometries of the neutral and cationic forms of the hydroxycarbenes by MP2/aug-cc-pVTZ. We used the equation-of-motion coupled-cluster method with single and double substitutions (EOM-CCSD). We computed vertical and adiabatic excitation energies, and oscillator strengths by EOM-EE-CCSD, and ionization energies (IEs) by EOM-IP-CCSD.[33−35] The aug-cc-pVTZ basis set was employed in all EOM calculations. Core electrons were frozen in all calculations. Our results agree well with previously reported results for HC and MHC of the excitation energies to S_1 and T_1, neutral and cation geometries, *cis*−*trans* energy gaps, and ionization energies (see Supporting Information for some comparisons).

To assign excited-state characters, we carried out NTO analyses of the EOM-EE-CCSD wave functions.[36−39] NTOs provide the most compact representation of the electronic transition. The NTO analysis allows one to easily determine the character of the transition, e.g., to distinguish between valence and Rydberg states, identify charge-transfer states, and assign specific character (n−n*, n−π*, etc.) to the transitions. We used the Gabedit interface to visualize the NTOs.

We assigned valence and Rydberg characters to the excited states by considering the symmetry of the transitions, the character of the NTOs, and the spatial extent of the particle orbitals [defined as the expectation value of the position operators, r_x, r_y, r_z; and the average radius of an orbital computed as $r = (r_x^2 + r_y^2 + r_z^2)^{0.5}$]. We also analyzed the Mulliken charge distributions in the ground and excited states. To compute adiabatic excitation energies for Rydberg states, we used the ground-state geometry of the cation, which is a common approximation.[40] For the valence states, we carried out geometry optimizations using EOM-EE-CCSD/aug-cc-pVTZ. Throughout the paper, the axis definition is the following: *X* and *Y* lie along the long and short axes of the molecule, respectively, and *Z* is perpendicular to the plane of the molecule. All the electronic structure calculations were carried out using Q-Chem.[41,42]

3. RESULTS AND DISCUSSION

3.1. Molecular Orbital Framework, Electronic Configurations, and Relevant Geometries. The bonding in hydroxycarbenes can be rationalized within the molecular orbital (MO) framework shown in Figure 1 for *trans*-HC. (A similar description applies to *cis*-HC.) The electronic configuration of HC in the ground electronic state can be written as

$$(1s_O)^2(1s_C)^2(\sigma_{OH})^2(\sigma_{CH})^2(LP_O)^2(\sigma_{CO})^2(\pi_{CO})^2(LP_C)^2$$

The electronic configuration of the lowest singlet and triplet excited states is

$$(1s_O)^2(1s_C)^2(\sigma_{OH})^2(\sigma_{CH})^2(LP_O)^2(\sigma_{CO})^2(\pi_{CO})^2(LP_C)^1(\pi^*_{CO})^1$$

DOI: 10.1021/acs.jpca.8b04424
J. Phys. Chem. A 2018, 122, 6176−6182

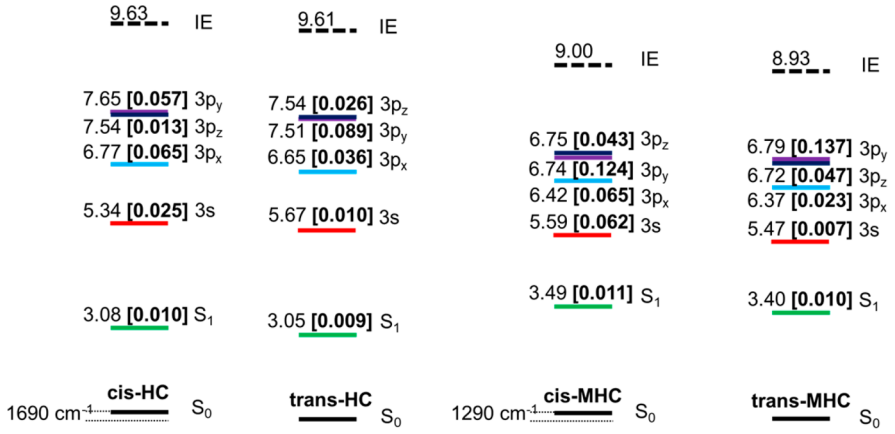

Figure 2. Vertical excitation energies and oscillator strengths calculated using EOM-CCSD/aug-cc-pVTZ for the *cis*- and *trans*-isomers of HC (left) and MHC (right). Vertical singlet electronic energies (regular font) and oscillator strengths (bold font, square bracket) are calculated at the ground-state optimized geometries. Vertical IE (black dashed line) and $\Delta E_{cis-trans}$ values are also shown.

While methylene has a triplet ground state with a vertical singlet−triplet gap of 0.2 eV,[43] hydroxycarbenes have singlet ground states resulting from the stabilizing interaction between the $2p_z$ orbital on carbon and the lone pair of oxygen.[44] Our calculations give vertical S−T gaps of 1.54 and 1.85 eV for HC and MHC, respectively; the corresponding adiabatic values are 1.07 and 1.27 eV. These values agree well with previously reported S−T gaps calculated at the CCSD(T)/aug-cc-pVnZ level for these carbenes (see Table S1 of the Supporting Information).

Section I in the Supporting Information shows the equilibrium structures of HC and MHC in their neutral, first excited singlet, and cationic states; these parameters agree well with previous studies.[23,24,26−28] In both carbenes, the *trans*-isomer is the most stable, and in Figure 2 we list the energy differences between the isomers of HC and MHC, which are in good agreement with previously published results.[45,46] The *cis*-isomers are higher in energy in both HC and MHC due to repulsive interactions between the oxygen lone pairs and the nonbonding carbon electrons.

3.2. Excited Electronic States. The vertical and adiabatic electronic excitation energies of the *cis*- and *trans*-isomers of HC and MHC, calculated by EOM-EE-CCSD, are summarized in Table 1 and Figure 2. Here we focus on the lowest-lying (n = 3) Rydberg states and their possible use for detection of hydroxycarbenes. For completeness we also report in Table S2 of the Supporting Information the vertical excitation energies and oscillator strengths of five A′ and five A″ excited singlet states up to the ionization energy. The S_1 energy of MHC is higher than that of HC due to the destabilization of the particle NTO (LUMO) by antibonding contributions from the C−H bonds of methyl (see Figure 3). The optimized relaxed geometry of S_1 involves a change in the H−O−C−C/H dihedral angle. This can be explained by considering changes in the nodal planes and overlap of the relevant molecular orbitals. In the planar ground-state geometry, the two filled lone pairs orbitals on oxygen are opposite in phase to the sp^2 hybridized lone pair orbitals on carbon. When the p-type LUMO on carbon is singly occupied in the S_1 state, rotation about the CO bond axis enhances the in-phase spatial overlap with the oxygen lone pairs, which has a stabilizing effect on S_1.[47] This is illustrated schematically in Figure S1 of the Supporting Information, which shows the increased in-phase orbital overlap in going from the C_s symmetry of S_0 to the C_1 symmetry of S_1. The explanation for the higher S−T gap for MHC follows the same reasoning, because T_1 has the same orbital configuration as S_1.

Table 1. Vertical and Adiabatic Excitation Energies of Singlet Rydberg States, Oscillator Strengths, and Quantum Defects for HC and MHC[a]

	state	E_{vert} (eV)	E_{adiab} (eV)	oscillator strength	quantum defect (δ)
		HC			
trans-HC	$2^1A'$ (3s)	5.67	4.87	0.010	1.141
	$3^1A'$ ($3p_x$)	6.65	5.96	0.036	0.856
	$4^1A'$ ($3p_y$)	7.51	6.88	0.089	0.454
	$2^1A''$ ($3p_z$)	7.54	6.86	0.026	0.436
	$1^2A'$ (IE)	9.61	8.94		
cis-HC	$2^1A'$ (3s)	5.34	4.76	0.025	1.219
	$3^1A'$ ($3p_x$)	6.77	6.01	0.065	0.818
	$4^1A'$ ($3p_y$)	7.65	6.93	0.057	0.378
	$2^1A''$ ($3p_z$)	7.54	6.81	0.013	0.448
	$1^2A'$ (IE)	9.63	8.91		
		MHC			
trans-MHC	$2^1A'$ (3s)	5.47	4.59	0.007	1.017
	$3^1A'$ ($3p_x$)	6.37	5.65	0.023	0.694
	$2^1A''$ ($3p_z$)	6.72	5.99	0.047	0.518
	$4^1A'$ ($3p_y$)	6.79	6.11	0.137	0.478
	$1^2A'$ (IE)	8.93	8.21		
cis-MHC	$2^1A'$ (3s)	5.59	4.80	0.085	1.002
	$3^1A'$ ($3p_x$)	6.42	5.62	0.073	0.703
	$2^1A''$ ($3p_z$)	6.74	6.03	0.051	0.546
	$4^1A'$ ($3p_y$)	6.75	6.08	0.130	0.540
	$1^2A'$ (IE)	9.00	8.24		

[a]Quantum defects are estimated from the Rydberg formula (see text).

The UV absorption spectra of HC and MHC measured in Ar matrix for the *trans*-isomers involve excitation to S_1.[23,24] The absorption spectrum of HC shows an onset at around 2.48 eV (500 nm) and a maximum at 2.90 eV (427 nm). The authors also report calculated adiabatic and vertical excitation energies to S_1 at 2.40 eV (516 nm) and 2.99 eV (415 nm), respectively.[23] These values are in excellent agreement with the adiabatic and vertical energies [excluding zero-point energy (ZPE) corrections] of 2.46 eV (504 nm) and 3.05 eV (406 nm), obtained in this work. The absorption spectrum of MHC shows an onset at around 460 nm and a maximum absorption

DOI: 10.1021/acs.jpca.8b04424
J. Phys. Chem. A 2018, 122, 6176−6182

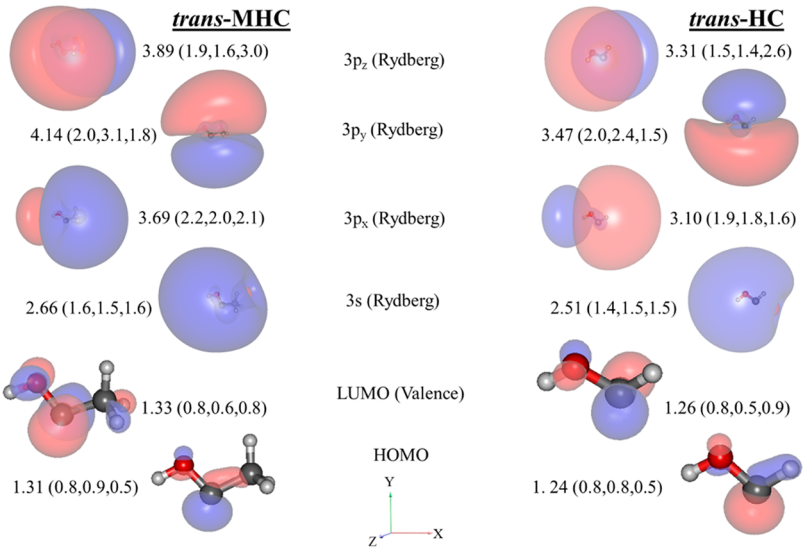

Figure 3. Particle NTOs and the hole NTO (labeled HOMO) for the lowest excited states of *trans*-MHC (left) and *trans*-HC (right). Their directional spatial extents in Å are labeled as r (r_x, r_y, r_z). The orientation of the molecules has been kept the same in all pictures.

at about 393 nm, and the calculated excitation energies to S_1 are 2.70 eV (459 nm) and 3.38 eV (367 nm) for the adiabatic and vertical transitions, respectively.[24] They agree with our calculations (excluding ZPE corrections) of 2.69 eV (461 nm) and 3.4 eV (365 nm), respectively. The broad absorption spectrum of HC shows several vibronic bands consistent with a change in the dihedral angle.[23] Moreover, the calculated oscillator strengths for the $S_1 \leftarrow S_0$ transitions of these carbenes are small (Figure 2 and Table 1), in agreement with experiments.[23,24] This is expected due to the poor overlap between the ground and excited-state electronic wave functions.

3.2.1. Cation and Rydberg States. Promotion of an electron from the nonbonding doubly occupied HOMO leads to a series of Rydberg states converging to the ground state of the cation. The vertical and adiabatic excitation energies for the n = 3 Rydberg manifold are summarized in Figure 2 and Table 1. The energy order of the states—a low-lying valence state, followed by the 3s, 3p$_x$, and nearly degenerate 3p$_y$ and 3p$_z$ states (in increasing order of energy)—does not change in going from HC to MHC and is the same for the *cis*- and *trans*-isomers. The electronic absorption spectrum of these carbenes is expected to be dominated by transitions to Rydberg states. Except for the S_1 state discussed above, no other singlet valence state was found near the n = 3 manifold. In fact, we found only one additional valence state, close to the IE, which does not mix with these states (see Table S2 in the Supporting Information). As expected, the IE of MHC is lower than that of HC due to hyperconjugation with the C−H bonds in the α-position, similar to the case for hydroxyalkyl radicals.[48]

The electronic excitation energies of the *trans*- and *cis*-isomers of the two carbenes are similar. The orientation of the O−H bond appears to have a minimal, if any, effect on the charge distribution in the ion core. In contrast to the trend in S_1, the Rydberg excitation energies of MHC are lower than those of HC. As discussed above, the lowering of the IE of MHC is caused by hyperconjugation that leads to stabilization of the cation.[48] As a result, its Rydberg series is lower in energy than in HC. Just the IE, however, does not explain the relative ordering of the 3p$_x$, 3p$_y$, and 3p$_z$ states. We find that the trends in relative ordering of the $3l_m$ Rydberg energies are similar for HC and MHC and for the *cis*- and *trans*-isomers, as discussed below.

The excitation energies of Rydberg states of small polyatomic molecules can be approximated by the Rydberg formula,

$$E_{ex} = \mathrm{IE} - \frac{\mathrm{Ryd}}{(n-\delta)^2}$$

where E_{ex} is the vertical excitation energy, IE is the vertical ionization energy of the molecule, Ryd = 13.61 eV is the Rydberg constant, n is the principal quantum number of the excited atomic orbital, and δ is the so-called quantum defect, which accounts for the interaction of the Rydberg electron with the cation core. The vertical E_{ex} energies obtained from the EOM-CCSD calculations were used in the Rydberg formula to obtain the δ values listed in Table 1. They represent the strength of the interaction with the ion core and depend on the shape and size of the ion core and the angular momentum of the participating orbitals. Typical values are δ = 0.9−1.2 for s states and 0.3−0.6 for p states. The quantum defect δ depends primarily on the size and shape of the ion core, whose geometry is similar to that of the cation. The IE of the molecule and the geometry of its cation are both determined by the redistribution of electron density in the ion core upon ionization. However, one should bear in mind that in neutral molecules Rydberg−valence interactions are common,[40] and can affect the geometry and electronic structure of the excited Rydberg state.

It is instructive to compare the δ values for the 3p Rydberg states of HC and MHC. Compared to states of the atoms, the Rydberg states of molecules have larger and more delocalized ion cores. While the nodes in the 3p orbitals are still centered on the C atom of the hydroxycarbenes, the Rydberg electron interacts with the entire ion core, and the strength of the electron−core interaction depends on the specific ion core charge distribution. The 3p$_x$ state is the most affected because it is exposed to the entirety of the positive charge along the C−O−H skeleton, defined here in the X direction. Indeed, the 3p$_x$ state has the highest quantum defect in both HC and MHC,

DOI: 10.1021/acs.jpca.8b04424
J. Phys. Chem. A 2018, 122, 6176−6182

with the largest δ value for HC. The positive charge distribution of the $3p_x$ ion core is directed toward H (in HC) and methyl (in MHC). However, the methyl group in MHC carries more of the positive charge than the sole hydrogen in HC. Naively, one would expect the additional methyl group to have an added contribution to the charge delocalization and thus to the quantum defect. However, two opposing factors come into play here. While the distribution of positive charge along several nuclei causes the Rydberg electron to interact with charges distributed over several atoms, as opposed to a single atom, the distribution of electron density throughout the core also induces greater screening by bonding and valence electrons, such as σ_{CC}. The final outcome is that the quantum defect of $3p_x$ is larger for HC than for MHC. Koziol et al.[49] explained the trends in quantum defects observed in a series of substituted vinyl radicals by similar arguments involving increased screening.

A clear distinction between Rydberg and valence orbitals is provided by inspection of the sizes of the NTOs shown in Figure 3. The energies and geometries of the S_1 states in HC and MHC were discussed above and illustrated by the particle NTO (which is similar to the LUMO). The HOMO and first excited valence orbital are of similar size (1.2−1.3 Å radius). The radius of the Rydberg orbitals ranges from 2.5 to 4.1 Å. It is useful to examine how the quantum defect manifests itself in the shapes of the Rydberg orbitals. The shapes are similar for both isomers (except for the $3p_y$ orbital discussed below), and therefore we use the orbitals of the *trans*-isomer as illustrative examples in Figure 3. The Rydberg orbital of the 3s state, the lowest in the series, is not as spherically symmetric as expected for an orbital with zero orbital angular momentum. The stronger interaction with the core reduces the size of this orbital compared to the size of the 3p orbitals and deforms its shape. The $3p_x$ orbital is deformed due to interactions with the ion core along the *X* axis. The $3p_y$ orbitals of the *trans*-isomer of HC and MHC are the most extended, because the single electron in the excited HOMO provides additional shielding from the positive core in the Y direction. As shown in Figure S2 in the Supporting Information, the shapes of the p_y orbitals of the *cis*- and *trans*-isomers of HC are slightly different. This is because the extent of the ion core in the *Y* direction changes slightly with the orientation of the OH bond.

3.2.2. Detection of Hydroxycarbenes. One of the goals of this study was to devise spectroscopic detection schemes for hydroxycarbenes. For molecular beam studies, the most sensitive technique is REMPI detection. Because their geometries are similar to those of the corresponding cations, Rydberg states often serve as intermediates in the initial excitation, followed by an efficient ionization step. Our results show that there are no valence states close in energy to the 3p Rydberg states. We expect only weak Rydberg−valence couplings,[40] and thus, REMPI detection via these states should be feasible.

In order to assess the detection sensitivity, we calculated the oscillator strengths of the transitions to the Rydberg states (see Table 1). One can rationalize the trends in the oscillator strength by inspection of the participating molecular orbitals. The NTOs in Figure 3 show that the ground-state orbital density of the lone pair on carbon is mostly distributed along the Y axis. Therefore, it is expected that the $3p_y$ state would have the highest oscillator strength in both HC and MHC. This is indeed the case for *trans*-HC and both isomers of MHC, where excitation to the $3p_y$ state has a much larger oscillator strength than the other states. In *cis*-HC, however, the oscillator strengths for transitions to $3p_y$ and $3p_x$ are comparable (see Table 1).

In deciding on the feasibility of detection schemes, the stability of the corresponding ion must be taken into account. Previous theoretical studies of the HC cation found a barrier of ∼25 kcal/mol for H elimination reaction.[9,50−52] The rearrangement barrier to the formaldehyde cation was found to be ∼50 kcal/mol. Similar studies of the MHC cation show a barrier height of ∼40 kcal/mol for isomerization to the acetaldehyde cation.[53−55] The barriers to hydrogen dissociation and isomerization to vinyl alcohol cation are about 30 kcal/mol. We conclude that the cations are fairly stable to dissociation and isomerization. The goal, therefore, is to first reach the Rydberg states and from there, assuming that the Rydberg ion core geometry is similar to that of the cation, we expect diagonal Franck−Condon factors for ionization.

An estimate of the Franck−Condon factors for excitation from the ground to the Rydberg state can be obtained from the calculated photoelectron spectrum of HCOH reported by Koziol et al.[28] They obtained vibronic progressions in the H−O−C and O−C−H bends, which is expected because in the cation the H−O−C and O−C−H angles are larger than in the ground state due to the increased s-type hybridization on C. In addition, the CO bond is shortened in the cation, which leads to a progression in the CO stretch. An absorption spectrum similar to the photoelectron spectrum is expected for the $3p_y$ and $3p_z$ states of HCOH, which have the smallest interactions with the core. Although similar calculations have not been reported for MHC, we expect a behavior similar to that of HC, because the geometry changes upon ionization are similar to those in HC. We believe that upon excitation to $3p_y$, vibrational progressions will be built on H−O−C and O−C−H bends and the CO stretch. The spectra, of course, will depend also on the internal energy of the generated carbenes, but the stability of the ion and the reasonable cross sections for excitation to the Rydberg states are promising for sensitive REMPI detection.

Based on the data summarized in Table 1, several detection schemes should be feasible for these carbenes. In using one-color schemes, we prefer that the excitation would reach not far above the ground state of the ion to avoid its dissociation. For HC a (2 + 1) REMPI scheme via the $3p_y$ state using 330−360 nm radiation should be feasible. Two color schemes are, of course, also possible with several different combinations. For MHC, a (1 + 1+1) REMPI scheme via the S_1 and $3p_y$ states can be achieved at 364−406 nm, and looks promising.

4. CONCLUSIONS

We report calculations of excited and ionized states of the *cis*- and *trans*-isomers of HC and MHC using EOM-CCSD and focusing on low-lying Rydberg states. Vertical and adiabatic excitation energies are reported along with the corresponding oscillator strengths for transitions from the ground electronic state. We describe the shapes and energy ordering of the low-lying Rydberg orbitals using NTO analysis and a simplified molecular orbital scheme. We also discuss the interaction of the Rydberg electrons with the ion core. Both HC and MHC have Rydberg 3p states in the 5−8 eV range, which can be accessed via multiphoton excitation schemes, and used for REMPI detection of this carbenes.

DOI: 10.1021/acs.jpca.8b04424
J. Phys. Chem. A 2018, 122, 6176−6182

■ ASSOCIATED CONTENT

Supporting Information

The Supporting Information is available free of charge on the ACS Publications website at DOI: 10.1021/acs.jpca.8b04424.

Relevant Cartesian geometries, S−T gaps, EOM-EE-CCSD state energies and oscillator strengths, illustration of orbital orientations in S_1, and NTOs of the *cis*-isomers (PDF)

■ AUTHOR INFORMATION

Corresponding Authors

*A. I. Krylov. E-mail: anna.i.krylov@gmail.com.
*H. Reisler. E-mail: reisler@usc.edu.

ORCID

Anna I. Krylov: 0000-0001-6788-5016
Hanna Reisler: 0000-0003-0176-6131

Notes

The authors declare no competing financial interest.

■ ACKNOWLEDGMENTS

B.R.S. acknowledges Sahil Gulania and Pavel Pohilko for helpful discussions. Computation for the work described in this paper was supported by the University of Southern California's Center for High-Performance Computing (hpcc.usc.edu). Support of the US Department of Energy, Basic Energy Sciences, Grant numbers DE-FG02-05ER15685 (A.I.K.) and DE-FG02-05ER15629 (H.R.) is gratefully acknowledged.

■ REFERENCES

(1) Bertrand, G. *Carbene Chemistry: From Fleeting Intermediates to Powerful Reagents*; CRC Press: Lausanne, Switzerland, 2002.
(2) Bourissou, D.; Guerret, O.; Gabbai, F. P.; Bertrand, G. Stable Carbenes. *Chem. Rev.* **2000**, *100*, 39−92.
(3) Baly, E. C. C.; Heilbron, I. M.; Barker, W. F. CX.—Photocatalysis. Part I. The Synthesis of Formaldehyde and Carbohydrates from Carbon Dioxide and Water. *J. Chem. Soc., Trans.* **1921**, *119*, 1025−1035.
(4) Kemper, M.; Van Dijk, J.; Buck, H. Ab Initio Calculation on the Photochemistry of Formaldehyde. The Search for a Hydroxycarbene Intermediate. *J. Am. Chem. Soc.* **1978**, *100*, 7841−7846.
(5) Shepler, B. C.; Epifanovsky, E.; Zhang, P.; Bowman, J. M.; Krylov, A. I.; Morokuma, K. Photodissociation Dynamics of Formaldehyde Initiated at the T_1/S_0 Minimum Energy Crossing Configurations. *J. Phys. Chem. A* **2008**, *112*, 13267−13270.
(6) Moore, C. B.; Weisshaar, J. C. Formaldehyde Photochemistry. *Annu. Rev. Phys. Chem.* **1983**, *34*, 525−555.
(7) Goddard, J. D.; Yamaguchi, Y.; Schaefer, H. F., III Features of the H_2CO Potential Energy Hypersurface Pertinent to Formaldehyde Photodissociation. *J. Chem. Phys.* **1981**, *75*, 3459−3465.
(8) Goddard, J. D.; Schaefer, H. F., III. The Photodissociation of Formaldehyde: Potential Energy Surface Features. *J. Chem. Phys.* **1979**, *70*, 5117−5134.
(9) Osamura, Y.; Goddard, J. D.; Schaefer, H. F., III; Kim, K. S. Near Degenerate Rearrangement Between the Radical Cations of Formaldehyde and Hydroxymethylene. *J. Chem. Phys.* **1981**, *74*, 617−621.
(10) Lucchese, R. R.; Schaefer, H. F., III Metal-Carbene Complexes and the Possible Role of Hydroxycarbene in Formaldehyde Laser Photochemistry. *J. Am. Chem. Soc.* **1978**, *100*, 298−299.
(11) Lahankar, S. A.; Chambreau, S. D.; Townsend, D.; Suits, F.; Farnum, J.; Zhang, X. B.; Bowman, J. M.; Suits, A. G. The Roaming Atom Pathway in Formaldehyde Decomposition. *J. Chem. Phys.* **2006**, *125*, 044303.
(12) Suits, A. G. Roaming Atoms and Radicals: A New Mechanism in Molecular Dissociation. *Acc. Chem. Res.* **2008**, *41*, 873−881.
(13) van Zee, R. D.; Foltz, M. F.; Moore, C. B. Evidence for a Second Molecular Channel in the Fragmentation of Formaldehyde. *J. Chem. Phys.* **1993**, *99*, 1664−1673.
(14) Wang, Y.; Bowman, J. M. Bend Excitation Is Predicted to Greatly Accelerate Isomerization of *trans*-Hydroxymethylene to Formaldehyde in the Deep Tunneling Region. *J. Phys. Chem. Lett.* **2015**, *6*, 124−128.
(15) Zhang, X.; Zou, S.; Harding, L. B.; Bowman, J. M. A Global ab Initio Potential Energy Surface for Formaldehyde. *J. Phys. Chem. A* **2004**, *108*, 8980−8986.
(16) Fu, B.; Shepler, B. C.; Bowman, J. M. Three-State Trajectory Surface Hopping Studies of the Photodissociation Dynamics of Formaldehyde on ab Initio Potential Energy Surfaces. *J. Am. Chem. Soc.* **2011**, *133*, 7957−7968.
(17) Shepler, B. C.; Braams, B. J.; Bowman, J. M. "Roaming" Dynamics in CH_3CHO Photodissociation Revealed on a Global Potential Energy Surface. *J. Phys. Chem. A* **2008**, *112*, 9344−9351.
(18) Bowman, J. M.; Shepler, B. C. Roaming Radicals. *Annu. Rev. Phys. Chem.* **2011**, *62*, 531−553.
(19) Feng, L.; Demyanenko, A. V.; Reisler, H. Competitive C−H and O−D Bond Fission Channels in the UV Photodissociation of the Deuterated Hydroxymethyl Radical CH_2OD. *J. Chem. Phys.* **2004**, *120*, 6524−6530.
(20) Feng, L.; Reisler, H. Photodissociation of the Hydroxymethyl Radical from the $2^2A''(3p_z)$ State: H_2CO and HCOH Products. *J. Phys. Chem. A* **2004**, *108*, 9847−9852.
(21) Rodrigo, C. P.; Sutradhar, S.; Reisler, H. Imaging Studies of Excited and Dissociative States of Hydroxymethylene Produced in the Photodissociation of the Hydroxymethyl Radical. *J. Phys. Chem. A* **2014**, *118*, 11916−11925.
(22) Rodrigo, C. P.; Zhou, C.; Reisler, H. Accessing Multiple Conical Intersections in the 3s and $3p_x$ Photodissociation of the Hydroxymethyl Radical. *J. Phys. Chem. A* **2013**, *117*, 12049−12059.
(23) Schreiner, P. R.; Reisenauer, H. P.; Pickard, F. C., IV; Simmonett, A. C.; Allen, W. D.; Mátyus, E.; Császár, A. G. Capture of Hydroxymethylene and Its Fast Disappearance Through Tunnelling. *Nature* **2008**, *453*, 906−909.
(24) Schreiner, P. R.; Reisenauer, H. P.; Ley, D.; Gerbig, D.; Wu, C.-H.; Allen, W. D. Methylhydroxycarbene: Tunneling Control of a Chemical Reaction. *Science* **2011**, *332*, 1300−1303.
(25) Leavitt, C. M.; Moradi, C. P.; Stanton, J. F.; Douberly, G. E. Helium Nanodroplet Isolation and Rovibrational Spectroscopy of Hydroxymethylene. *J. Chem. Phys.* **2014**, *140*, 171102.
(26) Koziol, L.; Wang, Y.; Braams, B. J.; Bowman, J. M.; Krylov, A. I. The Theoretical Prediction of Infrared Spectra of *trans*-and *cis*-Hydroxycarbene Calculated Using Full Dimensional ab Initio Potential Energy and Dipole Moment Surfaces. *J. Chem. Phys.* **2008**, *128*, 204310.
(27) Matus, M. H.; Nguyen, M. T.; Dixon, D. A. Heats of Formation and Singlet-Triplet Separations of Hydroxymethylene and 1-Hydroxyethylidene. *J. Phys. Chem. A* **2006**, *110*, 8864−8871.
(28) Koziol, L.; Mozhayskiy, V. A.; Braams, B. J.; Bowman, J. M.; Krylov, A. I. Ab Initio Calculation of the Photoelectron Spectra of the Hydroxycarbene Diradicals. *J. Phys. Chem. A* **2009**, *113*, 7802−7809.
(29) Back, R.; Yamamoto, S. The Gas-Phase Photochemistry and Thermal Decomposition of Glyoxylic Acid. *Can. J. Chem.* **1985**, *63*, 542−548.
(30) Yamamoto, S.; Back, R. The Photolysis and Thermal Decomposition of Pyruvic Acid in the Gas Phase. *Can. J. Chem.* **1985**, *63*, 549−554.
(31) Takahashi, K.; Plath, K. L.; Axson, J. L.; Nelson, G. C.; Skodje, R. T.; Vaida, V. Dynamics and Spectroscopy of Vibrational Overtone Excited Glyoxylic Acid and 2, 2−Dihydroxyacetic Acid in the Gas-Phase. *J. Chem. Phys.* **2010**, *132*, 094305.
(32) Takahashi, K.; Plath, K. L.; Skodje, R. T.; Vaida, V. Dynamics of Vibrational Overtone Excited Pyruvic Acid in the Gas Phase: Line Broadening Through Hydrogen-Atom Chattering. *J. Phys. Chem. A* **2008**, *112*, 7321−7331.

DOI: 10.1021/acs.jpca.8b04424
J. Phys. Chem. A 2018, 122, 6176−6182

(33) Bartlett, R. J. Coupled-Cluster Theory and Its Equation-of-Motion Extensions. Wiley Interdiscip. *Rev. Comput. Mol. Sci.* **2012**, *2*, 126−138.
(34) Krylov, A. I. Equation-of-Motion Coupled-Cluster Methods for Open-Shell and Electronically Excited Species: The Hitchhiker's Guide to Fock Space. *Annu. Rev. Phys. Chem.* **2008**, *59*, 433−462.
(35) Sneskov, K.; Christiansen, O. Excited State Coupled Cluster Methods. *Wiley Interdiscip. Rev. Comput. Mol. Sci.* **2012**, *2*, 566−584.
(36) Luzanov, A.; Sukhorukov, A.; Umanskii, V. Application of Transition Density Matrix for Analysis of Excited States. *Theor. Exp. Chem.* **1976**, *10*, 354−361.
(37) Mewes, S. A.; Plasser, F.; Krylov, A.; Dreuw, A. Benchmarking Excited-State Calculations Using Exciton Properties. *J. Chem. Theory Comput.* **2018**, *14*, 710−725.
(38) Plasser, F.; Bäppler, S. A.; Wormit, M.; Dreuw, A. New Tools for the Systematic Analysis and Visualization of Electronic Excitations. II. Applications. *J. Chem. Phys.* **2014**, *141*, 024107.
(39) Plasser, F.; Wormit, M.; Dreuw, A. New Tools for the Systematic Analysis and Visualization of Electronic Excitations. I. Formalism. *J. Chem. Phys.* **2014**, *141*, 024106.
(40) Reisler, H.; Krylov, A. I. Interacting Rydberg and Valence States in Radicals and Molecules: Experimental and Theoretical Studies. *Int. Rev. Phys. Chem.* **2009**, *28*, 267−308.
(41) Krylov, A. I.; Gill, P. M. Q-Chem: An Engine for Innovation. *Wiley Interdiscip. Rev. Comput. Mol. Sci.* **2013**, *3*, 317−326.
(42) Shao, Y.; Gan, Z.; Epifanovsky, E.; Gilbert, A. T.; Wormit, M.; Kussmann, J.; Lange, A. W.; Behn, A.; Deng, J.; Feng, X.; et al. Advances in Molecular Quantum Chemistry Contained in the Q-Chem 4 Program Package. *Mol. Phys.* **2015**, *113*, 184−215.
(43) Vargas, R.; Galván, M.; Vela, A. Singlet-Triplet Gaps and Spin Potentials. *J. Phys. Chem. A* **1998**, *102*, 3134−3140.
(44) Mueller, P. H.; Rondan, N. G.; Houk, K.; Harrison, J. F.; Hooper, D.; Willen, B. H.; Liebman, J. F. Carbene Singlet-Triplet Gaps. Linear Correlations with Substituent π Donation. *J. Am. Chem. Soc.* **1981**, *103*, 5049−5052.
(45) Evanseck, J.; Houk, K. Theoretical Predictions of Activation Energies for 1,2-Hydrogen Shifts in Singlet Carbenes. *J. Phys. Chem.* **1990**, *94*, 5518−5523.
(46) Räsänen, M.; Raaska, T.; Kunttu, H.; Murto, J. Ab Initio Studies on Carbenes; Singlet and Triplet Conformers and Vibrational Spectra of Hydroxy-, Dihydroxy- and Methylhydroxy-Carbene. *J. Mol. Struct.: THEOCHEM* **1990**, *208*, 79−90.
(47) Hwang, D.-Y.; Mebel, A. M.; Wang, B.-C. Ab Initio Study of the Addition of Atomic Carbon with Water. *Chem. Phys.* **1999**, *244*, 143−149.
(48) Karpichev, B.; Reisler, H.; Krylov, A. I.; Diri, K. Effect of Hyperconjugation on Ionization Energies of Hydroxyalkyl Radicals. *J. Phys. Chem. A* **2008**, *112*, 9965−9969.
(49) Koziol, L.; Levchenko, S. V.; Krylov, A. I. Beyond Vinyl: Electronic Structure of Unsaturated Propen-1-yl, Propen-2-yl, 1-Buten-2-yl, and *trans*-2-Buten-2-yl Hydrocarbon Radicals. *J. Phys. Chem. A* **2006**, *110*, 2746−2758.
(50) Bouma, W. J.; Macleod, J. K.; Radom, L. An Ab Initio Molecular Orbital Study of the $CH_2O^{+\bullet}$ Isomers: The Stability of the Hydroxymethylene Radical Cation. *Int. J. Mass Spectrom. Ion Phys.* **1980**, *33*, 87−93.
(51) Burgers, P. C.; Mommers, A. A.; Holmes, J. Ionized Oxycarbenes: Hydroxymethylidyne Cation ($[COH]^+$), Hydroxymethylene Cation ($[HCOH]^{+\bullet}$), Dihydroxymethylene Cation ($[C(OH)_2]^{+\bullet}$), Formoxylium Cation ($[HCO_2]^+$) and Carboxyl Cation ($[COOH]^+$), Their Generation, Identification, Heat of Formation, and Dissociation Characteristics. *J. Am. Chem. Soc.* **1983**, *105*, 5976−5979.
(52) Wagner, J. P.; Bartlett, M. A.; Allen, W. D.; Duncan, M. A. Tunneling Isomerizations on the Potential Energy Surfaces of Formaldehyde and Methanol Radical Cations. *ACS Earth Space Chem.* **2017**, *1*, 361−367.
(53) Apeloig, Y.; Karni, M.; Ciommer, B.; Depke, G.; Frenking, G.; Meyn, S.; Schmidt, J.; Schwarz, H. $[CH_3COH]^{\bullet+}$, the Central Intermediate in the Isomerization-Dissociation Reactions of Ionized Vinyl Alcohol. *J. Chem. Soc., Chem. Commun.* **1983**, *0*, 1497−1499.
(54) Smith, B. J.; Nguyen, M. T.; Bouma, W. J.; Radom, L. Unimolecular Rearrangements Connecting Hydroxyethylidene (CH_3-C-OH), Acetaldehyde (CH_3-CH = O), and Vinyl Alcohol (CH_2=CH-OH). *J. Am. Chem. Soc.* **1991**, *113*, 6452−6458.
(55) Terlouw, J. K.; Wezenberg, J.; Burgers, P. C.; Holmes, J. L. New, Stable Isomers of $[C_2H_4O]^{+\bullet}$, and $[C_2H_4O_2]^{+\bullet}$, the Radical Cations $[CH_3COH]^{+\bullet}$ and $[CH_3OCOH]^{+\bullet}$. *J. Chem. Soc., Chem. Commun.* **1983**, 1121−1123.

DOI: 10.1021/acs.jpca.8b04424
J. Phys. Chem. A 2018, 122, 6176−6182